Available online at www.sciencedirect.com

ScienceDirect

www.elsevier.com/locate/jes

JES JOURNAL OF ENVIRONMENTAL SCIENCES

www.jesc.ac.cn

Effect of barium sulfate modification on the SO_2 tolerance of V_2O_5/TiO_2 catalyst for NH_3-SCR reaction

Tengfei Xu[1], *Xiaodong Wu*[1,2,*], *Xuesong Liu*[3], *Li Cao*[1], *Qiwei Lin*[4], *Duan Weng*[1]

1. *Key Laboratory of Advanced Materials of Ministry of Education, School of Materials Science and Engineering, Tsinghua University, Beijing 100084, China. E-mail: xtf14@mails.tsinghua.edu.cn*
2. *Yangtze Delta Region Institute of Tsinghua University, Jiaxing 314006, China*
3. *College of Chemistry and Chemical Engineering, Shaoxing University, Shaoxing 312000, China*
4. *Redbud Innovation Institute, Longyan, Fujian 364000, China*

ARTICLE INFO

Article history:
Received 14 November 2016
Revised 25 November 2016
Accepted 29 November 2016
Available online 6 December 2016

Keywords:
SCR catalyst
Sulfur poisoning
Barium sulfate
Decomposable sulfate

ABSTRACT

Sulfur poisoning of $V_2O_5/BaSO_4$–TiO_2 (VBT), V_2O_5/WO_3–TiO_2 (VWT) and $V_2O_5/BaSO_4$–WO_3–TiO_2 (VBWT) catalysts was performed in wet air at 350°C for 3 hr, and activities for the selective catalytic reduction of NO_x with NH_3 were evaluated for 200–500°C. The VBT catalyst showed higher NO_x conversions after sulfur poisoning than the other two catalysts. The introduction of barium sulfate contributed to strong acid sites for the as-received catalyst, and eliminated the redox cycle of active vanadium oxide to some extent, which resulted in a certain loss of activity. Readily decomposable sulfate species formed on VBT-S instead of inactive sulfates on VWT-S. These decomposable sulfates increased the number of strong acid sites significantly. Some sulfate species escaped during catalyst preparation and barium sulfate was reproduced during sulfur poisoning, which protects vanadia from sulfur oxide attachment to a great extent. Consequently, the VBT catalyst exhibited the best resistance to sulfur poisoning.

Introduction

Nitrogen oxides (NO_x) that are emitted from fossil combustion are a major source of air pollution. Because of their large-scale emissions, NO_x reduction has become an important issue. The selective catalytic reduction of NO with NH_3 (NH_3-SCR) in the presence of excess oxygen is a widely used technology to remove NO_x from flue gases of power boilers and industrial furnaces (Liu et al., 2013; Nie et al., 2014; Chen et al., 2015a, 2015b; Ma et al., 2015; Maitarad et al., 2016; Geng et al., 2016). V_2O_5/WO_3–TiO_2 catalyst, a well-known commercial catalyst, has been used for decades owing to its stability and high catalytic activity at 300–400°C (Pan et al., 2013; Zhang et al., 2015). However, this catalyst still experiences some drawbacks, such as a high cost of tungsten oxide as additive and a relatively low sulfur tolerance in high-SO_2 concentration atmospheres.

Nowadays an important promoter for commercial V_2O_5/TiO_2 is tungsten oxide, which can enhance SCR performance by increasing the Brönsted acid sites and the redox property of the VO_x species (Cheng et al., 2014; Kwon et al., 2016). The phase transition of anatase to rutile can be inhibited with tungsten oxide addition (Paganini et al., 1997; Liu and Woo, 2006; Kubacka et al., 2014). However, tungsten oxide introduction has little effect on SO_2 tolerance enhancement and even increases SO_2 oxidation to SO_3 to some extent by the promoted dispersion of vanadia (Koppula et al., 1998; Kwon et al., 2016). SO_2 can be oxidized to SO_3 by dispersed vanadia species to form metal sulfates, which may block catalyst pore channels or eliminate

* *Corresponding author*. E-mail: wuxiaodong@tsinghua.edu.cn (Xiaodong Wu).

http://dx.doi.org/10.1016/j.jes.2016.12.001
1001-0742/

the redox cycle of active sites, which leads to a decrease in SCR catalyst activity (Liu et al., 2011).

An enhanced or reduced catalytic performance by the sulfate species formed on the catalyst depends on their nature and properties (Chen and Yang, 1990; Topsoe et al., 1995; Wang et al., 2015). Significant effort has been devoted to improving the sulfur tolerance of V_2O_5/TiO_2 catalysts in the past decade (Li et al., 2014; Yang et al., 2016). Orsenigo et al. reported that sulfation was preferable on vanadium oxide rather than tungsten oxide and titanium dioxide (Orsenigo et al., 1998), which was also confirmed by our previous work (Chen et al., 2015a, 2015b). Khodayari et al. found that sulfate species formed after sulfur poisoning could strengthen active Brönsted acid sites and increase and stabilize catalytic activity (Khodayari and Odenbrand, 2001). Muhammad et al. introduced CeO_2 to $Sb\text{-}V_2O_5/TiO_2$, and found that Ce(III) sulfate that formed at high temperatures was more active for NH_3-SCR than Ce(IV) sulfate formed at low temperatures (Maqbool et al., 2014).

The roles of barium oxide and barium sulfate have been studied for sulfur resistance in NO_x storage reduction catalysts (Su and Amiridis, 2004; Elbouazzaoui et al., 2005; Corbos et al., 2008; Tanaka et al., 2013). Well-dispersed barium sulfate that is located in the Pt proximity is more reducible than bulk-like species at low temperature (Poulston and Rajaram, 2003; Elbouazzaoui et al., 2005; Wei et al., 2005). The introduction of barium sulfate could increase NO_x adsorption and resistance to SO_2 over $Pt/CeO_2–ZrO_2$ catalyst, which could promote the decomposition of deposited sulfates and reduce sulfur species accumulation (Corbos et al., 2008; Zheng et al., 2012).

We lreport a novel strategy to obtain a high-SO_2-resistant V_2O_5/TiO_2 catalyst by modification with low-cost barium sulfate, which is of significant importance for possible industrial applications. Fresh and sulfated catalysts were characterized by X-ray diffraction (XRD), Brunner–Emmett–Teller surface area (BET), thermogravimetric analysis (TGA), inductively coupled plasma (ICP), temperature-programmed desorption/reduction (TPD/R) and NH_3 temperature-programmed desorption (NH_3-TPD).

1. Experimental

1.1. Catalyst preparation

$BaSO_4–WO_3–TiO_2$ (BWT) mixed oxides were prepared by mixing aqueous solutions of metatitanic acid (Beijing Chem, Beijing, China), ammonium paratungstate (Beijing Chem, Beijing, China) and barium sulfate in a weight ratio of $WO_3:BaSO_4:TiO_2$ = 1.25:1.25:97.5. The obtained mixtures were stirred for 1 hr, and the solution was titrated with 15 wt.% ammonia hydroxide (Beijing Chem, Beijing, China) until the pH reached 9. The resulting precipitates were dried at 80°C overnight and calcined at 500°C for 3 hr in air. $WO_3–TiO_2$ (WT) and $BaSO_4–TiO_2$ (BT) powders with $WO_3:TiO_2$ = 2.5:97.5 and $BaSO_4:TiO_2$ = 2.5:97.5 were prepared by the same method. $V_2O_5/BaSO_4–WO_3–TiO_2$ (VBWT), $V_2O_5/WO_3–TiO_2$ (VWT) and $V_2O_5/BaSO_4–TiO_2$ (VBT) catalysts were prepared by an incipient wetness impregnation method on the corresponding supports. The nominal loading amount of vanadia was 1 wt.% using an ammonium metavanadate precursor (Beijing Chem, Beijing, China). The paste was dried at 110°C overnight and calcined at 450°C for 3 hr.

Sulfur poisoning was performed by exposing the as-received catalysts to a stream of 1000 ppm SO_2, 20% O_2, 10% H_2O and a balance of N_2 in a fixed-bed quartz tube at 350°C for 3 hr, and the corresponding sulfated catalysts were denoted VBWT-S, VWT-S and VBT-S.

1.2. Activity measurement

NH_3-SCR activity measurements were carried out in a fixed-bed quartz tube at the 200–500°C. The reactor containing 200 mg catalyst (60–80 mesh) with a GHSV (Reactant Gas Flow Rate/Reactor Volume) of 12,000 hr^{-1}. The feed stream consisted of 500 ppm NH_3, 500 ppm NO, 250 ppm SO_2, 5% O_2 and a balance of N_2 (500 mL/min). The outlet gas was monitored at 150°C by using a Thermo Nicolet 380 FTIR spectrometer (Thermo Nicolet 380 FTIR spectrometer, Thermo Fisher Scientific, USA) equipped with 2 m path length sample cell (250 mL volume). The NO_x conversion and N_2 selectivity were calculated as Eqs. (1) and (2), respectively.

$$NO_x\ \text{conversion}(\%) = \frac{[NO]_{in}-[NO]_{out}-[NO_2]_{out}-2[N_2O]_{out}}{[NO]_{in}} \times 100 \quad (1)$$

$$N_2\ \text{selectivity}(\%) = \left(1-\frac{[NO_2]_{out}+2[N_2O]_{out}}{[NH_3]_{in}+[NO]_{in}-[NH_3]_{out}-[NO]_{out}}\right) \times 100 \quad (2)$$

1.3. Catalyst characterization

Catalyst powder XRD patterns were determined by using a D/mas-RB diffractometer (Rigaku, Tokyo, Japan) at 40 kV and 120 mA with Cu K_α radiation (λ = 0.15418 nm). The patterns were recorded at 0.02° intervals for $20° \le 2\theta \le 70°$ with a scanning velocity of 4°/min.

The catalyst specific surface area was measured by using N_2 adsorption at −196°C by the four-point BET method using an automatic surface analyzer (F-Sorb 3400, Gold APP, China). Prior to the analysis, catalysts were degassed in vacuum at 200°C for 2 hr.

The thermo gravimetric analysis (TGA) of the catalysts was performed on a Mettler Toledo TGA/DSC instrument from room temperature to 1100°C in N_2 (50 mL/min) at 10°C/min. Approximately 10 mg catalyst was weighed onto an alumina pan for each test.

ICP analysis was carried out using an ICP emission spectrometer (Vista-MPX, Varian, USA).

H_2 temperature-programmed reduction (H_2-TPR) was conducted on a Micromeritics AutoChem II 2920 (AutoChem II 2920, Micromeritics, USA). Prior to the conventional H_2-TPR run, 50 mg catalyst was treated in He at 300°C for 30 min. The catalyst was heated to 900°C at 10°C/min in 10% H_2/Ar (50 mL/min) with the H_2 consumption recorded by TCD. The outlet gases were also detected by a mass spectrometer (Mass spectrometer, Omnistar 200, Germany). Another H_2-TPR was carried out after TPR pretreatment and isothermal oxidation. Firstly, the catalyst was heated in 10% H_2/Ar to 500°C at 10°C/min to remove

decomposable sulfates. Isothermal oxidation pretreatment was carried out in 10% O_2/He at 500°C for 30 min and the catalyst was cooled to room temperature before H_2-TPR was performed.

NH_3 temperature-programmed desorption (NH_3-TPD) was performed in a fixed-bed quartz tube. The catalyst was pretreated at 500°C for 1 hr in 8% O_2/N_2 (500 mL/min) stream. After cooling to room temperature, the catalyst was exposed to 500 ppm NH_3/N_2 (500 mL/min) until saturation, followed by purging with N_2 for 30 min. The catalyst was heated to 500°C at 10°C/min in N_2 (500 mL/min). The outlet NH_3 concentration was monitored by a Nicolet 380 spectrometer.

2. Results

2.1. Catalytic activities

Fig. 1a compares the NH_3-SCR activities of the fresh catalysts. They followed the order VWT > VBWT > VBT at low temperatures ($T \leq 300$°C) and VBWT ≈ VBT > VWT at high temperatures ($T \geq 400$°C). The fresh VWT catalyst showed higher deNO_x efficiency than the other two catalysts at low temperature, which implies a lowered reactivity of vanadia species from the interaction with barium sulfate. Catalysts exhibited higher activities at high temperatures with barium sulfate addition. As shown in Fig. 1c, almost no NO_2 was detected in the downstream gas in the entire temperature region. However, the increase in N_2O production becomes obvious at the temperatures higher than 400°C, resulting in a decrease in N_2 selectivity. The addition of barium sulfate does not appear to change the selectivity to N_2.

Under real working conditions, especially in coal-fired power plants, exhaust gases always contain some SO_2 and H_2O (Srivastava et al., 2004). Thus, the NH_3-SCR activities of the catalysts after 3 hr wet sulfur poisoning have been studied and the results are shown in Fig. 1b and d. The SO_2 deactivation effect was serious for VWT, which showed a significant decrease in low-temperature activity and high-temperature N_2 selectivity. It is unusual to find that both the activity and selectivity of VBT-S catalyst are enhanced. Therefore, the substation of tungsten oxide by barium sulfate promotes the SO_2 resistance of vanadia based catalysts.

2.2. XRD and BET

XRD patterns of the catalysts are shown in Fig. 2. All catalysts exhibited typical anatase TiO_2 structural features. No WO_3, V_2O_5 or $Ti(SO_4)_2$ diffraction peaks were detected, which suggests that these metal oxides and sulfate were well dispersed or amorphous in the catalysts (ARATA et al., 1990; Sohn et al., 2002; Yu et al.,

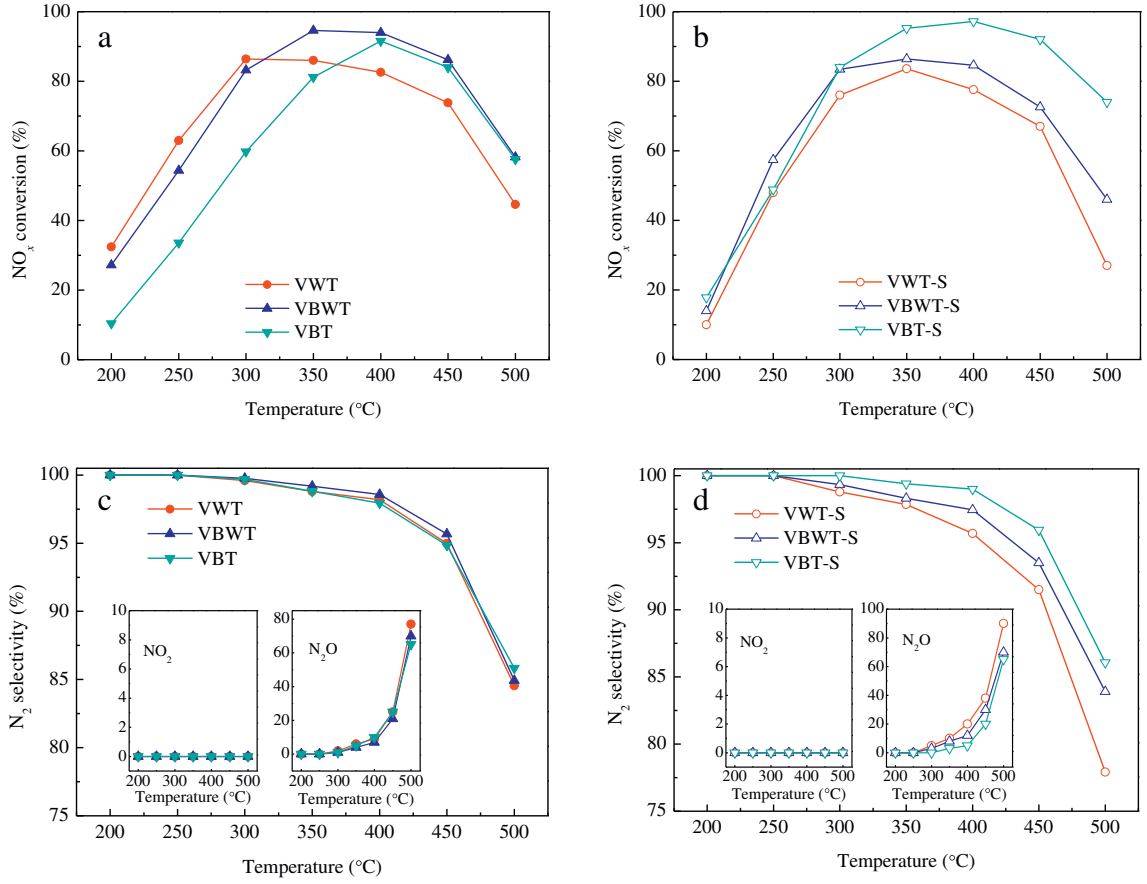

Fig. 1 – (a, b) NO_x conversion and (c, d) N_2 selectivity over the fresh and poisoned catalysts for NH_3-SCR. Reaction conditions: NO = NH_3 = 500 ppm, SO_2 = 250 ppm, O_2 = 5%, N_2 in balance, GHSV = 12,000 hr^{-1}. NO_x: nitrogen oxides; NH_3-SCR: selective catalytic reduction of NO with NH_3.

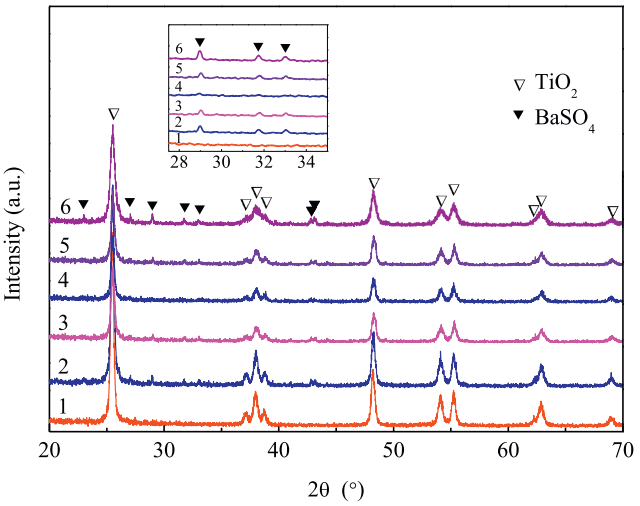

Fig. 2 – XRD patterns of (1) VWT, (2) VBWT, (3) VBT, (4) VWT-S, (5) VBWT-S and (6) VBT-S catalysts. XRD: X-ray diffraction; VWT: $V_2O_5/WO_3–TiO_2$; VBWT: $V_2O_5/BaSO_4–WO_3–TiO_2$; VBT: $V_2O_5/BaSO_4–TiO_2$.

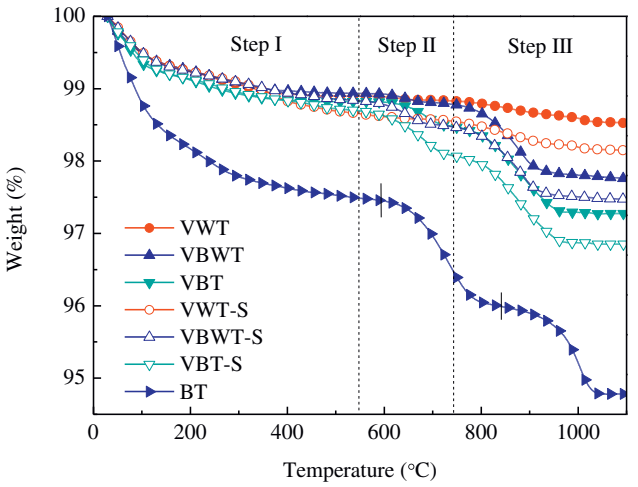

Fig. 3 – TGA curves of catalysts in N_2. TGA: thermogravimetric analysis.

2013). Some weak barium sulfate diffraction peaks were visible in the XRD patterns of the catalysts that contained barium sulfate, as shown in the inset in Fig. 2. These results suggest that barium sulfate exists in the prepared catalysts using $BaSO_4$ as a precursor after calcination. Additionally, the diffraction peaks of barium sulfate increased in intensity after sulfur poisoning, which implies that more barium sulfate formed during treatment.

The catalyst surface areas are listed in Table 1. The introduction of barium sulfate to the catalysts does not affect the catalyst surface area significantly. The specific surface area of the catalyst decreased after sulfur poisoning, because of the blockage of catalyst pore channels by deposited sulfates (Liu et al., 2011).

2.3. TGA and ICP

Sulfate deposition is important in the catalytic performance of poisoned catalysts, and TGA and ICP analyses have been applied to determine the amount of sulfates over different catalysts. TGA curves of the catalysts are shown in Fig. 3, and the mass losses are summarized in Table 2. All catalysts revealed certain mass losses for 25–545, 545–745 and 745–1100°C. The mass loss of step I is ascribed to the loss of water and easily decomposable impurities in the catalysts. The mass losses of steps II and III were assigned to the decomposition of surface and bulk sulfate species, which corresponds to the decomposition of BT (Corbos et al., 2008). The readily decomposable sulfate species, as will be discussed in the H_2-TPR results, decomposed at step II in N_2, whereas the decomposition of strongly-interacted sulfates such as vanadium sulfate occurred at higher temperatures (step III). The differences in catalyst mass loss (Δ) before and after sulfur poisoning were calculated, which could indicate the amount of decomposable sulfates deposited on the catalysts. The result followed the order of VBT-S > VBWT-S > VWT-S at step II and a reverse sequence at step III. This implies that the majority of sulfates on VBWT-S and especially VBT-S were readily decomposable sulfates, whereas those on VWT-S were more stable bulk sulfates, including strongly-interacted vanadium sulfate. The ICP results are listed in Table 2. The increased S contents in the poisoned catalysts are similar to each other. By assuming no loss of sulfur upon catalyst preparation, the theoretical sulfur contents in the fresh VBWT and VBT should be 0.51% and 1.02%, respectively, which is much larger than the S values detected by ICP. These results confirm barium sulfate decomposition and sulfate radical loss upon calcination during catalyst preparation. An increased mass loss of VBT-S at steps II and III (0.283%) is ascribed to the deposited sulfate decomposition. This corresponds to an S content of 0.1142% if we assume that the deposition of sulfates generates SO_3 or $SO_2 + 1/2O_2$, which is similar to the TG result. Thus, it can be deduced that sulfates deposited on VBT-S can be decomposed even in N_2. However, those on VWT-S can be decomposed less easily.

Table 1 – Textural, redox and acidic properties of catalysts.

Catalysts	S_{BET} (m^2/g)	H_2 consumption [a] (μmol/g)	NH_3 desorption [b] (μmol/g)
VWT(-S)	54 (43)	170 (70)	99 (113)
VBWT(-S)	56 (42)	166 (85)	134 (154)
VBT(-S)	58 (46)	130 (110)	158 (186)

[a] Calculated by integrating areas of desorption peaks in Fig. 7.
[b] Calculated by integrating areas of reduction peaks at 370–400°C in Fig. 6.

2.4. Redox property

The availability and amount of redox sites on the fresh and sulfated catalysts was determined by using H_2-TPR. The profiles obtained are shown in Fig. 4. The VWT catalyst showed three reduction peaks centered at 400, 436 and 776°C. The first peak is ascribed to the reduction of $V^{5+} \rightarrow V^{3+}$ (Yu et al., 2013; Chen et al., 2015a, 2015b; Ma et al., 2015). The second and third peaks correspond to the successive reduction of $W^{6+} \rightarrow W^{4+}$ and

Table 2 – Mass losses and S contents of catalysts.

Catalyst	Weight loss at Step II (wt.%) [a]	Δ at Step II (wt.%) [a]	Weight loss at Step III (wt.%) [a]	Δ at Step III (wt.%) [a]	Decomposable sulfate content (wt.%) [b]	S content (wt.%) [c]	Δ_S (wt.%) [c]
VWT	0.066	–	0.302	–	–	0.03	–
VBWT	0.158	–	1.015	–	–	0.18	–
VBT	0.349	–	1.196	–	–	0.28	–
VWT-S	0.106	0.040	0.403	0.101	0.141	0.16	0.13
VBWT-S	0.364	0.206	1.024	0.009	0.215	0.30	0.12
VBT-S	0.627	0.278	1.201	0.005	0.283	0.39	0.11

VWT: $V_2O_5/WO_3–TiO_2$; VBWT: $V_2O_5/BaSO_4–WO_3–TiO_2$; VBT: $V_2O_5/BaSO_4–TiO_2$.
[a] Measured by TGA (thermogravimetric analysis).
[b] Calculated by assumption.
[c] Measured by ICP (inductively coupled plasma).

$W^{4+} \rightarrow W^0$, respectively (Wang et al., 2013). These reduction peaks shifted towards lower temperatures with the addition of barium sulfate especially for VBT. However, they do not imply an increase in vanadia and tungsten oxide species reducibility because of interference from the decomposition and reduction of sulfates.

To confirm the influence of sulfate decomposition/reduction on the hydrogen consumption of catalysts, the production of SO_2 and H_2S was monitored by MS and the results are shown in Fig.5. The H_2S peak at 370°C is attributed to the reduction of surface barium sulfate, which contributes significantly to the first reduction peak of VBT in Fig. 4. Similarly, the release of SO_2 at 367°C is ascribed to the decomposition of barium sulfate, which also contributes to the H_2 reduction peak at 367°C. The simultaneous appearance of a H_2 consumption peak for BT at 561°C in Fig. 4 and a SO_2 peak in Fig. 5b indicates their direct relationship, which was caused by surface barium sulfate (Wei et al., 2005). However, the reduction peak of barium sulfate can shift to 385°C after loading vanadia. A similar promoting effect of Pt and Rh on the decomposition of surface barium sulfate has been reported by Wei et al. (2005). The interference of sulfate reduction/decomposition is more significant for the catalysts after sulfur poisoning.

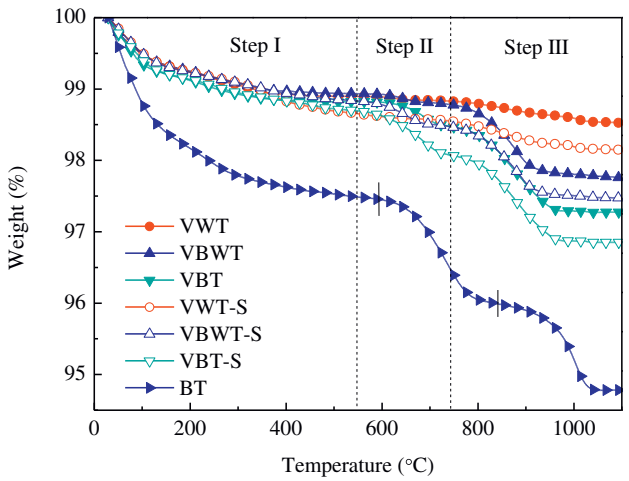

Fig. 4 – Conventional H_2-TPR catalyst profiles. H_2-TPR: H_2 temperature-programmed reduction.

The redox properties of vanadia species are critical to the catalyst SCR activity. To avoid the influence of sulfates, fresh and poisoned catalysts were pretreated in H_2 by running TPR from room temperature to 500°C and these were oxidized in O_2 at 500°C for 30 min. After such desulfation treatment, no

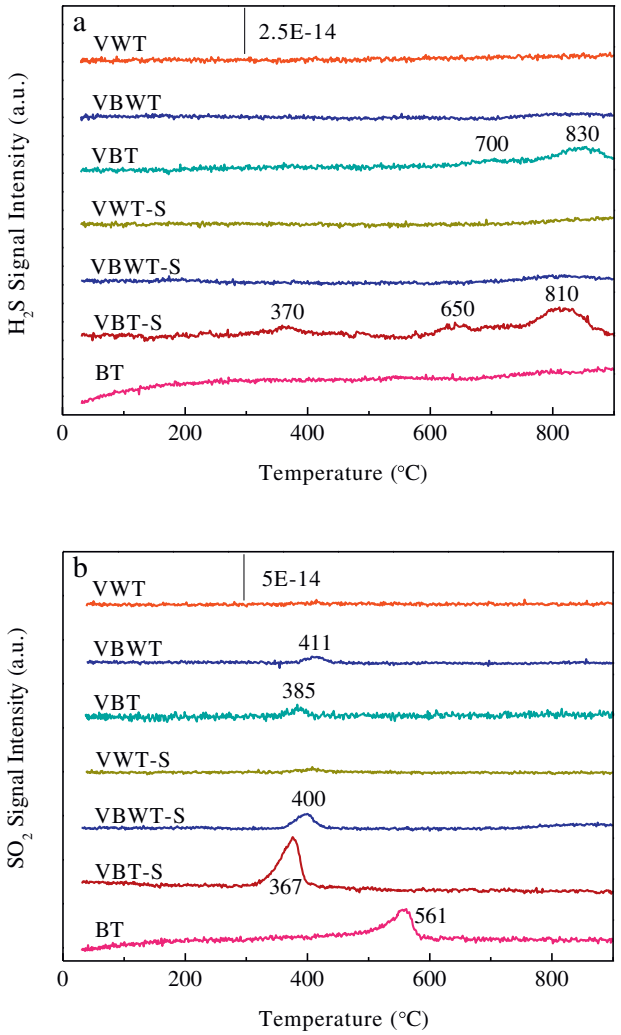

Fig. 5 – Evolutions of outlet (a) H_2S and (b) SO_2 signal for conventional catalyst H_2-TPR tests. H_2-TPR: H_2 temperature-programmed reduction.

H_2S or SO_2 signal was detected by MS when performing H_2-TPR tests, which indicates the complete removal of decomposable/reducible sulfates. Although vanadia species do not remain in the same state after pretreatment, the redox property of catalysts is suggested not to change significantly because only those reducible sulfates were removed. As shown in Fig. 6, the reduction peak was deconvoluted into two overlapped peaks centered at 400 (370 for VBT-S) and 435°C, which is ascribed to the reduction of $V^{5+} \rightarrow V^{3+}$ and $W^{6+} \rightarrow W^{4+}$, respectively. The H_2 consumption values of the first peak, which represent the amount of active vanadia species quantitatively (Zhao et al., 2010), are summarized in Table 1. The amount of active vanadia on the WT support decreases by ~60% after sulfur poisoning, whereas the drop is only 15% for VBT-S. The decrease in H_2 consumption is caused by a strong interaction between vanadium and sulfate species, which cuts off the redox cycle in the NH_3-SCR reaction and leads to catalyst deactivation. The replacement of a WT support by BT results in the decrease of vanadia species reducibility on the fresh sample. However, most active vanadia is preserved on VBT-S, whereas the loss of active metal oxides is most severe on VWT-S. The above results are consistent with low-temperature catalyst activities, which demonstrate the importance of active vanadia in the SCR reaction.

2.5. NH_3-TPD

Because NH_3 absorption/desorption is a critical process in NH_3-SCR, NH_3-TPD was performed to measure the amount and strength of acid sites on the catalyst surface (Zhihua Lian et al., 2015). The results are shown in Fig. 7 and the total NH_3 desorption values as estimated by integrating the peak areas are listed in Table 1. All catalysts showed two overlapping peaks with the first at 100–280°C (weak acid sites) and the second at 280–450°C (strong acid sites) (Maqbool et al., 2014). The total amount of NH_3 desorbed followed the order VBT > VBWT > VWT for the fresh catalysts. The amount of desorbed NH_3 increased in the presence of barium sulfate, especially at high temperature, which means that more acid sites exist on catalysts that contain sulfate species than on VWT. NH_3 desorption of the catalysts increases after sulfur poisoning, which suggests that the sulfate deposited on the catalysts can serve as strong acid sites for NH_3 adsorption.

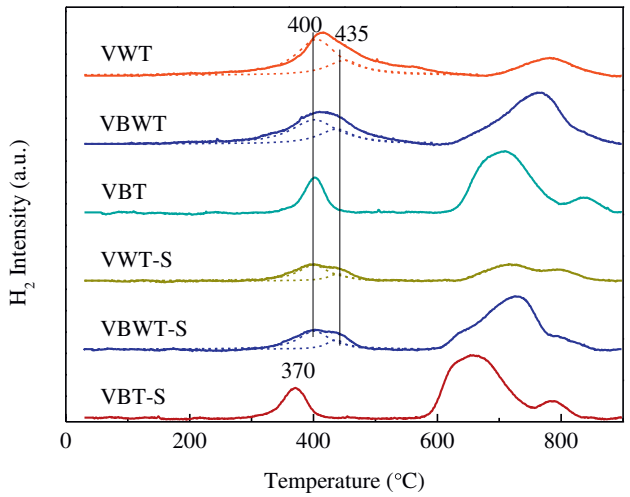

Fig. 6 – H_2-TPR profiles after desulfation treatment. H_2-TPR: H_2 temperature-programmed reduction.

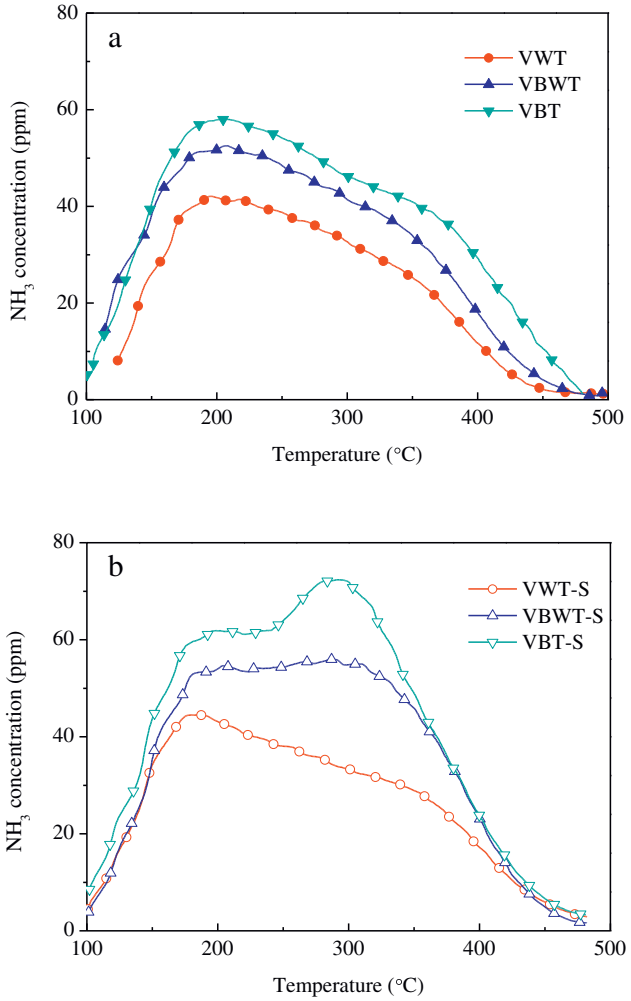

Fig. 7 – NH_3-TPD profiles of (a) fresh and (b) sulfur-poisoned catalysts. NH_3-TPD: NH_3 temperature-programmed desorption.

3. Discussion

3.1. *Influence of sulfur poisoning on structure and sulfate species*

Although the introduction of barium sulfate does not yield any obvious effect on catalyst surface area, some vanadium oxide interacted with the sulfate radical from barium sulfate, which is consistent with a decrease in H_2 consumption for the VBT catalyst (Fig. 6), and results in a poor VBT catalyst SCR activity at low temperature. As shown by the ICP results, some sulfate species were lost from the as-prepared catalyst during calcination. This implies that some barium may exist as BaO or other species that are in too low concentrations to be

detected by XRD. These non-sulfates appeared to react with SO_3 to form barium sulfate again upon sulfur poisoning, which is evidenced by the increase in intensity of barium sulfate characteristic peaks in the XRD pattern of the VBT-S catalyst. As a result, most vanadia is conserved because of the sacrificing effect of these barium species. Although the ICP results indicate that the amounts of deposited sulfates are similar on different sulfated catalysts, their decomposition behaviors are rather different based on the TGA results. More readily decomposable sulfates existed on VBWT-S and especially VBT-S. The ratio of decomposable sulfates is lowest and they tend to decompose at high temperature on VWT-S, which implies a stronger interaction from sulfate species on VWT-S. The SO_2 deactivation mechanisms over different catalysts are shown in Scheme 1. The non-sulfate barium species types and their possible transformation during a durability test remain to be identified.

3.2. *Effect of sulfur poisoning on surface acidity and redox property*

It has been reported that the surface acidity and redox property play dominant roles in NH_3-SCR performance (Peng et al., 2013; Li et al., 2015; Qu et al., 2016; Zhang et al., 2016). In general, the redox property can be evaluated by H_2-TPR, which is affected by the reduction of doped/deposited sulfates. A so-called redox pretreatment was attempted to exclude the influence of decomposable sulfates, and the reactivity of active vanadia species was expressed as an integrated area of the first deconvoluted reduction peak in H_2-TPR profile. After the addition of barium sulfate, the reducibility of VBT decreased to some extent, which may be because of the interaction of the introduced vanadia and sulfate species. This weakened reducibility should account for the lower NH_3-SCR activity of the VBT catalyst at low temperature. After sulfur poisoning, the reducibility decreased sharply for the VWT-S catalyst, which resulted from the formation of stable metal sulfates, including vanadium sulfate. It is important to establish only a small decrease in H_2 consumption of the first deconvoluted reduction peak for the VBT-S catalyst, which suggests that it still exhibited a good reducibility after sulfur poisoning. The catalyst surface acidity is determined by NH_3-TPD. The addition of barium sulfate increases the surface acidity of the fresh catalyst VBT. Similarly, the deposited sulfates also contributed to the surface acidity of the sulfated catalysts, which was consistent with Khodayari's investigation that the introduced sulfates increased the strength of the surface acid site and the catalytic activity (Khodayari and Odenbrand, 2001). Combined with the TGA results, it is reasonable to believe that decomposable sulfates acts as important strong acid sites, which facilitates the SCR reaction at high temperatures, and contributes to low-temperature activity.

4. Conclusions

The effects of barium sulfate in V_2O_5/TiO_2-based catalysts on the NH_3-SCR activity and sulfur resistance were investigated. The addition of barium sulfate into the titania support instead of tungsten oxide can enhance the SO_2 tolerance significantly. According to the TGA and H_2-TPR results, the vanadia on VWT-S interacted strongly with sulfate species to form stable vanadium sulfate, which resulted in a significant decrease in NO_x conversion from 87% to 75% at 300°C. Although a similar amount of sulfates was deposited on the VBT-S catalyst, they are decomposable species that contribute to a significant increase in strong acid sites but also do not inhibit active vanadia reactivity. As a result, NO_x conversion over VBT-S increased from 62% to 85% at 300°C and reached a maximum (96%) at 400°C. The $V_2O_5/BaSO_4$–TiO_2 catalyst appears to be a promising NH_3-SCR catalyst for application in SO_2-containing exhaust emissions.

Acknowledgments

The authors would like to acknowledge the financial support from projects of the Ministry of Science and Technology, China (Nos. 2015AA034603, 2016YFC0205200) and the Science and Technology Department of Zhejiang Province, China (No. 2015C31015).

REFERENCES

ARATA, K., HINO, M., YAMAGATA, N., 1990. Acidity and catalytic activity of zirconium and titanium sulfates heat-treated at high-temperature. Solid superacid catalysts. Bull. Chem. Soc. Jpn. 63 (1), 244–246.

Chen, J.P., Yang, R.T., 1990. Mechanism of poisoning of the V_2O_5/TiO_2 catalyst for the reduction of NO by NH_3. J. Catal. 125, 411–420.

Chen, L., Si, Z., Wu, X., Weng, D., Wu, Z., 2015b. Effect of water vapor on NH_3-NO/NO_2 SCR performance of fresh and aged MnO_x–NbO_x–CeO_2 catalysts. J. Environ. Sci. 31, 240–247.

Chen, C., Wu, X., Yu, W., Gao, Y., Weng, D., Shi, L., et al., 2015a. Potassium poisoning of titania supported deNO_x catalysts:

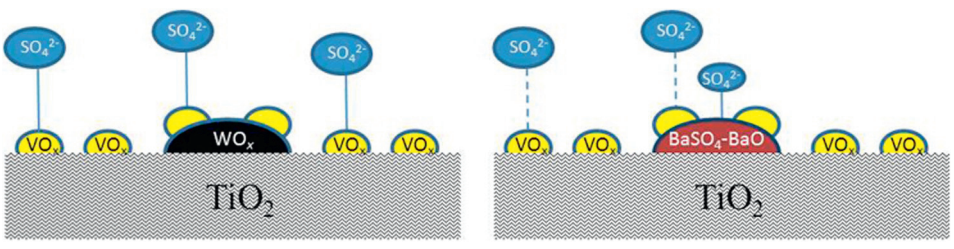

Scheme 1 – SO_2 deactivation mechanisms over different catalysts.

preservation of vanadia and sacrifice of tungsten oxide. Chin. J. Catal. 36 (8), 1287–1294.
Cheng, K., Liu, J., Zhang, T., Li, J., Zhao, Z., Wei, Y., et al., 2014. Effect of Ce doping of TiO_2 support on NH_3-SCR activity over V_2O_5-WO_3/CeO_2-TiO_2 catalyst. J. Environ. Sci. 26 (10), 2106–2113.
Corbos, E.C., Courtois, X., Bion, N., Marecot, P., Duprez, D., 2008. Impact of the support oxide and Ba loading on the sulfur resistance and regeneration of Pt/Ba/support catalysts. Appl. Catal. B 80 (1–2), 62–71.
Elbouazzaoui, S., Corbos, E.C., Courtois, X., Marecot, P., Duprez, D., 2005. A study of the deactivation by sulfur and regeneration of a model NSR Pt/Ba/Al_2O_3 catalyst. Appl. Catal. B 61 (3–4), 236–243.
Geng, Y., Shan, W., Xiong, S., Liao, Y., Yang, S., Liu, F., 2016. Effect of CeO_2 for a high-efficiency CeO_2/WO_3–TiO_2 catalyst on N_2O formation in NH_3-SCR: a kinetic study. Catal. Sci. Technol. 6 (9), 3149–3155.
Khodayari, R., Odenbrand, C.U.I., 2001. Regeneration of commercial SCR catalysts by washing and sulphation: effect of sulphate groups on the activity. Appl. Catal. B 33, 277–291.
Koppula, P.R., Dunn, J.P., Stenger, H.G., Wachs, I.E., 1998. Oxidation of sulfur dioxide to sulfur trioxide over supported vanadia catalysts. Appl. Catal. B 19, 103–117.
Kubacka, A., Lglesias-Juez, A., Michiel, M., Becerro, A.I., Fernandez-Garcia, M., 2014. Morphological and structural behavior of TiO_2 nanoparticles in the presence of WO_3: crystallization of the oxide composite system. Phys. Chem. Chem. Phys. 16 (36), 19540–19549.
Kwon, D.W., Park, K.H., Hong, S.C., 2016. Enhancement of SCR activity and SO_2 resistance on VO_x/TiO_2 catalyst by addition of molybdenum. Chem. Eng. J. 284, 315–324.
Li, X., Li, J., Peng, Y., Zhang, T., Liu, S., Hao, J., 2015. Selective catalytic reduction of NO with NH_3 over novel iron–tungsten mixed oxide catalyst in a broad temperature range. Catal. Sci. Technol. 5 (9), 4556–4564.
Li, P., Liu, Z., Li, Q., Wu, W., Liu, Q., 2014. Multiple roles of SO_2 in selective catalytic reduction of NO by NH_3 over V_2O_5/AC catalyst. Ind. Eng. Chem. Res. 53 (19), 7910–7916.
Lian, Z., Liu, F., He, H., Liu, K., 2015. Nb-doped VO_x/CeO_2 catalyst for NH_3-SCR of NO_x at low temperatures. RSC Adv. 5 (47), 37675–37681.
Liu, Z., Woo, S.I., 2006. Recent advances in catalytic DeNO_x science and technology. Catal. Rev. 48 (1), 43–49.
Liu, F., Asakura, K., He, H., Shan, W., Shi, X., Zhang, C., 2011. Influence of sulfation on iron titanate catalyst for the selective catalytic reduction of NO_x with NH_3. Appl. Catal. B 103 (3–4), 369–377.
Liu, F., Shan, W., Lian, Z., Xie, L., Yang, W., He, H., 2013. Novel $MnWO_x$ catalyst with remarkable performance for low temperature NH_3-SCR of NO_x. Catal. Sci. Technol. 3 (10), 2699–2707.
Ma, Z., Wu, X., Feng, Y., Si, Z., Weng, D., Shi, L., 2015. Low-temperature SCR activity and SO_2 deactivation mechanism of Ce-modified V_2O_5–WO_3/TiO_2 catalyst. Prog. Nat. Sci. 25 (4), 342–352.
Maitarad, P., Meeprasert, J., Shi, L., Limtrakul, J., Zhang, D., Namuangruk, S., 2016. Mechanistic insight into the selective catalytic reduction of NO by NH_3 over low-valent titanium-porphyrin: a DFT study. Catal. Sci. Technol. 6 (11), 3878–3885.
Maqbool, M.S., Pullur, A.K., Ha, H.P., 2014. Novel sulfation effect on low-temperature activity enhancement of CeO_2-added Sb-V_2O_5/TiO_2 catalyst for NH_3-SCR. Appl. Catal. B 152-153, 28–37.
Nie, J., Wu, X., Ma, Z., Xu, T., Si, Z., Chen, L., et al., 2014. Tailored temperature window of MnO_x-CeO_2 SCR catalyst by addition of acidic metal oxides. Chin. J. Catal. 35 (8), 1281–1288.
Orsenigo, C., Lietti, L., Tronconi, E., Forzatti, P., Bregani, F., 1998. Dynamic investigation of the role of the surface sulfates in NO_x reduction and SO_2 oxidation over V_2O_5–WO_3/TiO_2 catalysts. Ind. Eng. Chem. Res. 37, 2350–2359.
Paganini, M.C., Dall'Acqua, L., Giamello, E., Lietti, L., Forzatti, P., Busca, G., 1997. An EPR study of the surface chemistry of the V_2O_5–WO_3/TiO_2 catalyst: redox behaviour and state of V(IV). J. Catal. 166, 195–205.
Pan, Y., Zhao, W., Zhong, Q., Cai, W., Li, H., 2013. Promotional effect of Si-doped V_2O_5/TiO_2 for selective catalytic reduction of NO_x by NH_3. J. Environ. Sci. 25 (8), 1703–1711.
Peng, Y., Qu, R., Zhang, X., Li, J., 2013. The relationship between structure and activity of MoO_3-CeO_2 catalysts for NO removal: influences of acidity and reducibility. Chem. Commun. 49 (55), 6215–6217.
Poulston, S., Rajaram, R.R., 2003. Regeneration of NO_x trap catalysts. Catal. Today 81 (4), 603–610.
Qu, R., Peng, Y., Sun, X., Li, J., Gao, X., Cen, K., 2016. Identification of the reaction pathway and reactive species for the selective catalytic reduction of NO with NH_3 over cerium–niobium oxide catalysts. Catal. Sci. Technol. 6 (7), 2136–2142.
Sohn, J.R., Kim, J.-G., Kwon, T.-D., Park, E.H., 2002. Characterization of titanium sulfate supported on zirconia and activity for acid catalysis. Langmuir 18, 1666–1673.
Srivastava, R.K., Miller, C.A., Erickson, C., Jambhekar, R., 2004. Emissions of sulfur trioxide from coal-fired power plants. J. Air Waste Manage. Assoc. 54 (6), 750–762.
Su, Y., Amiridis, M.D., 2004. In situ FTIR studies of the mechanism of NO_x storage and reduction on Pt/Ba/Al_2O_3 catalysts. Catal. Today 96 (1–2), 31–41.
Tanaka, T., Amano, K., Dohmae, K., Takahashi, N., Shinjoh, H., 2013. Studies on the regeneration of sulfur-poisoned NO_x storage and reduction catalysts, including a Ba composite oxide. Appl. Catal. A 455, 16–24.
Topsoe, N.-Y., Dumesic, J.A., Topsoe, H., 1995. Vanadia/titania catalysts for selective catalytic reduction of nitric oxide by ammonia. J. Catal. 151, 241–252.
Wang, Y., Li, X., Zhan, L., Li, C., Qiao, W., Ling, L., 2015. Effect of SO_2 on activated carbon honeycomb supported CeO_2–MnO_x catalyst for NO removal at low temperature. Ind. Eng. Chem. Res. 54 (8), 2274–2278.
Wang, C., Yang, S., Chang, H., Peng, Y., Li, J., 2013. Dispersion of tungsten oxide on SCR performance of $V_2O_5WO_3$/TiO_2: acidity, surface species and catalytic activity. Chem. Eng. J. 225, 520–527.
Wei, X., Liu, X., Deeba, M., 2005. Characterization of sulfated BaO-based NO_x trap. Appl. Catal. B 58 (1–2), 41–49.
Yang, W., Liu, F., Xie, L., Lian, Z., He, H., 2016. Effect of V_2O_5 additive on the SO_2 resistance of a Fe_2O_3/AC catalyst for NH_3-SCR of NO_x at low temperatures. Ind. Eng. Chem. Res. 55 (10), 2677–2685.
Yu, W., Wu, X., Si, Z., Weng, D., 2013. Influences of impregnation procedure on the SCR activity and alkali resistance of V_2O_5–WO_3/TiO_2 catalyst. Appl. Surf. Sci. 283, 209–214.
Zhang, L., Li, L., Cao, Y., Yao, X., Ge, C., Gao, F., et al., 2015. Getting insight into the influence of SO_2 on TiO_2/CeO_2 for the selective catalytic reduction of NO by NH_3. Appl. Catal. B 165, 589–598.
Zhang, T., Qiu, F., Chang, H., Li, X., Li, J., 2016. Identification of active sites and reaction mechanism on low-temperature SCR activity over Cu-SSZ-13 catalysts prepared by different methods. Catal. Sci. Technol. http://dx.doi.org/10.1039/c6cy00737f.
Zhao, H., Bennici, S., Cai, J., Shen, J., Auroux, A., 2010. Effect of vanadia loading on the acidic, redox and catalytic properties of V_2O_5–TiO_2 and V_2O_5–TiO_2/SO_4^{2-} catalysts for partial oxidation of methanol. Catal. Today 152 (1–4), 70–77.
Zheng, Y., Zheng, Y., Xiao, Y., Cai, G., Wei, K.-M., 2012. Effect of barium sulfate on sulfur resistance of Pt/$Ce_{0.4}Zr_{0.6}O_2$ catalyst. Catal. Commun. 27, 189–192.